

Toluene Solubilization Induces Different Modes of Mixed Micelle Growth[†]

Yael G. Mishael and Paul L. Dubin*

Department of Chemistry, Indiana University-Purdue University, Indianapolis, Indiana 46202

Received February 25, 2005. In Final Form: April 14, 2005

The effect of toluene solubilization on the size and mobility of Triton X100 (TX100) micelles and TX100/sodium dodecyl sulfate (SDS) mixed micelles was studied by turbidimetry, dynamic light scattering, and capillary electrophoresis. Micelle growth due to toluene solubilization was observed for both surfactant systems; however, two different modes of growth were seen. Mixed micelles in 0.1 M NaCl are spherical (apparent diameter $d_{app} = 8$ nm) and remain so while taking up 3 mM toluene, with a volume increase per micelle of $\Delta V_m = 50$ nm³. In 0.5 M NaCl, the large d_{app} of both nonionic and mixed micelles (14 and 24 nm, respectively) indicate ellipsoidal or rodlike shapes, and their large increases in d_{app} upon addition of 3 mM toluene thus correspond to elongational growth, with the same $\Delta V_m = 50$ nm³. Further addition of toluene to TX100/SDS in 0.5 M NaCl results in a dramatic increase in micelle size followed by an unexpected bimodal size distribution. The addition of excess toluene leads to the formation of ca. 140 nm toluene droplets, stabilized mainly by monomers of the high critical micelle concentration surfactant, SDS. These microemulsions coexist with the smaller (20 nm) swollen mixed micelles.

Introduction

The phenomenon of solubilization, increasing the solubility of an insoluble or poorly soluble organic substance in a surfactant solution, is widely studied and well established.^{1–6} Research efforts have focused on quantifying solubilization by determining the partition constant (solubilization coefficient) which describes the solubilization distribution between the micelle and bulk phases.^{7–11} Solubilization studies have also focused on the effect of external factors such as ionic strength^{1,12–14} and temperature.^{11,15} Attempts to elucidate the mechanism of solu-

bilization have involved studies of solubilization location inside micelles.^{6,16–19} Such research complements applications of micellar solubilization in several fields such as cosmetics, pharmaceuticals, and detergency in general.

A variety of new environmental applications are increasingly based on solubilization of organic pollutants. Most research and field tests throughout the past decade have focused on “enhanced pump and treat” remediation techniques also known as “soil flushing”.^{20–22} This technique aims to improve the removal of trapped nonaqueous liquids during the pumping process by solubilization of the trapped pollutants. Successful field demonstrations have resulted. With the goal of improving the understanding of “enhanced pump and treat”, solubilization coefficients have been calculated for several pollutants.^{16,23–27} In contrast to the preceding aquifer treatment, a more novel method, micelle-enhanced ultrafiltration,

* To whom the correspondence should be addressed: Department of Chemistry, 402 N. Blackford St., Indianapolis, IN 46202-3274; phone, 317-274-6872; fax, 317-274-4701; e-mail, dubin@chem.iupui.edu.

[†] Part of the Bob Rowell Festschrift special issue.

(1) Elworthy, P. H.; Florence, A. T.; Macfarlane, C. B. *Solubilization by surface-active agents*; Chapman and Hall, Ltd.: London, 1968.

(2) Dunaway, C. S.; Christian, S. D.; Scamehorn, J. F. *Surf. Sci. Ser.* **1995**, *55* (Solubilization in Surfactant Aggregates), 3–31.

(3) Rosen, M. J. *Surface and Interfacial Phenomena*; Wiley and Sons: New York, 1978.

(4) Scamehorn, J. F.; Harwell, J. H. Surfactants in Emerging Technologies. In *Surfactant Science Series*; Rosen, M. J., Ed.; Marcel Dekker: New York, 1987; Vol. 26, p 169.

(5) Zana, R. *Adv. Colloid Interface Sci.* **1995**, *57*, 1–64.

(6) Nagarajan, R.; Ruckenstein, E. *Langmuir* **1991**, *7* (12), 2934–69.

(7) Kawamura, H.; Manabe, M.; Miyamoto, Y.; Fujita, Y.; Tokunaga, S. *J. Phys. Chem.* **1989**, *93* (14), 5536–40.

(8) Edwards, D. A.; Luthy, R. G.; Liu, Z. *Environ. Sci. Technol.* **1991**, *25* (1), 127–33.

(9) Marangoni, D. G.; Kwak, J. C. T. *Langmuir* **1991**, *7* (10), 2083–8.

(10) Morgan, M. E.; Uchiyama, H.; Christian, S. D.; Tucker, E. E.; Scamehorn, J. F. *Langmuir* **1994**, *10* (7), 2170–6.

(11) Sakulwongyai, S.; Trakultamupatam, P.; Scamehorn, J. F.; Osuwan, S.; Christian, S. D. *Langmuir* **2000**, *16* (22), 8226–8230.

(12) Israelachvili, J. N. *Intermolecular and Surface Forces*; Academic Press: Sydney, 1985; pp 229–262.

(13) Ikeda, S.; Maruyama, Y. *J. Colloid Interface Sci.* **1994**, *166* (1), 1–5.

(14) Kim, J.-H.; Domach, M. M.; Tilton, R. D. *Langmuir* **2000**, *16* (26), 10037–10043.

(15) Wang, Z.; Zhao, F.; Li, D. *Huagong Xuebao* **2003**, *54* (10), 1387–1390.

(16) Diallo, M. S.; Abriola, L. M.; Weber, W. J., Jr. *Environ. Sci. Technol.* **1994**, *28* (11), 1829–37.

(17) Guha, S.; Jaffe, P. R.; Peters, C. A. *Environ. Sci. Technol.* **1998**, *32* (7), 930–935.

(18) Hawrylak, B.; Gracie, K.; Palepu, R. *Can. J. Chem.* **1998**, *76* (4), 464–468.

(19) Hedin, N.; Sitnikov, R.; Furo, I.; Henriksson, U.; Regev, O. *J. Phys. Chem. B* **1999**, *103* (44), 9631–9639.

(20) West, C. C.; Harwell, J. H. *Environ. Sci. Technol.* **1992**, *26* (12), 2324–30.

(21) Jafvert, C. T. *Surfactants/Cosolvents*; TE-96-02; December 1996.

(22) Harwell, J. H.; Sabatini, D. A.; Knox, R. C. *Colloids Surf., A* **1999**, *151* (1–2), 255–268.

(23) Pennell, K. D.; Adinolfi, A. M.; Abriola, L. M.; Diallo, M. S. *Environ. Sci. Technol.* **1997**, *31* (5), 1382–1389.

(24) Zimmerman, J. B.; Kibbey, T. C. G.; Cowell, M. A.; Hayes, K. F. *Environ. Sci. Technol.* **1999**, *33* (1), 169–176.

(25) Cowell, M. A.; Kibbey, T. C. G.; Zimmerman, J. B.; Hayes, K. F. *Environ. Sci. Technol.* **2000**, *34* (8), 1583–1588.

(26) Liu, G. G.; Roy, D.; Rosen, M. J. *Langmuir* **2000**, *16* (8), 3595–3605.

(27) Hill, A. J.; Ghoshal, S. *Environ. Sci. Technol.* **2002**, *36* (18), 3901–3907.

remediates water by forcing it through an ultrafiltration membrane with pore sizes small enough to block passage of the micelles and associated pollutants.^{28,29} Less developed are those aquifer methods known as “permeable reactive barriers”. While these involve many interactions with a variety of substrates, solubilization forms the basis of a recently proposed permeable reactive barrier, based on siliceous surfaces pretreated with a polycation that attaches oppositely charged mixed micelles which can solubilize a variety of pollutants.³⁰ Evidently, environmental applications involving micelles depend on a fundamental understanding of solubilization.

There are relatively few studies that report micelle size as a function of solubilize in support of the common assumption that micelles swell due to solubilization. In contrast, micelle growth due to an increase in ionic strength or concentration has been thoroughly studied. Stephany et al.³¹ used dynamic and static light scattering to measure changes in size and shape of sodium dodecyl sulfate (SDS) micelles caused by the addition of 1-pentanol at different ionic strengths. The addition of small amounts of alcohol produced an increase in micelle hydrodynamic radius: a sphere to rod transition at low ionic strength, and elongation of rodlike micelles at high ionic strength. A subsequent study by the same group indicated that pentanol isomers produced a similar effect, the magnitude of which depended on both the isomer and the temperature.³² Menge et al.^{33,34} studied the molar mass of micelles of the nonionic surfactant C₁₂E₅ in the presence of decane. They reported an increase in the molar mass with an increase in decane content and a transition from elongated micelles to microemulsion droplets at high decane concentrations. A similar transition from elongated micelles to microemulsion droplets for the C₁₆TABB/benzene system was suggested based on measurements of the field-dependent ²H spin relaxation of benzene.¹⁹ Kim et al.¹⁴ studied the effect of electrolytes on the capacity of SDS micelles for pyrene, i.e., the average number of pyrene molecules solubilized at saturation in a single SDS micelle. They concluded that capacity increases significantly when the micelle aggregation number changes in response to changing ionic strength or upon alteration of counterion binding affinity. However, solubilization power, the number of molecules solubilized per molecule of surfactant, was only weakly dependent on the factors mentioned above. Changes in micelle size and shape during solubilization lead to changes in the system properties, for example in viscosity and conductivity.³⁵ Because these properties have an impact on surfactant performance in many applications, further studies on solubilization-induced micelle swelling are valuable.

The examination of micelle swelling should include mixed micelles, rather than pure species, since the former are used in most applications: surfactant mixtures are usually less expensive, reduce the total monomer con-

centration, and often perform better, i.e., “synergistic behavior”.³⁶ In addition, mixed micelle properties can be tuned through the surfactant ratio. Mixed micelles are likely to be compositionally heterogeneous, i.e., possessing a broad distribution of microscopic micelle compositions,³⁷ and this heterogeneity may lead to a nonuniform solubilization that is a distribution of solubilization capacities. Therefore, we found it essential to obtain a better understanding of solubilization-induced micelle growth in a mixed micelle system. We studied the effect of toluene, a model organic pollutant, on TX100/SDS mixed micelles, as a function of ionic strength, the ratio of surfactants, and the total surfactant concentration. Micelle hydrodynamic diameters were followed using dynamic light scattering (DLS), and micelle mobility was measured by capillary electrophoresis.

Materials and Methods

Materials. Sodium dodecyl sulfate (SDS) was from Fisher Scientific Co. (FairLawn NJ), Triton X100 (TX100), toluene, and mesityl oxide were from Aldrich (Milwaukee, WI), and boric acid was from Sigma (St. Louis, MO). Milli-Q water was used throughout this study.

Turbidimetry. Pure toluene (0–40 mM) was added to solutions of 60 mM TX100 in 0.5 M NaCl, and transmittance was measured after the solutions were agitated overnight. Solutions of TX100 (10, 40, and 60 mM) in 0.5 M NaCl and of SDS/TX100 (15, 30, 60, and 90 mM) surfactant in 0.16 and 0.5 M NaCl were titrated with increments of 0.02 mL of pure toluene in intervals of 0.5 min. Transmittance was measured after each addition of toluene. Transmittance measurements were obtained at 420 nm with a Brinkmann (Westbury, NY) PC800 probe colorimeter with an effective path length of 2 cm. Values are reported as 100 – %*T*, which varies linearly with the true turbidity at low values of 100 – %*T*, and in a more complex manner at higher values.

Dynamic Light Scattering (DLS). Solutions of TX100 and TX100/SDS were prepared at 10–60 mM total surfactant concentration in 0.5 M and/or in 0.1 M NaCl. The ratio of SDS in the mixed micelles was kept constant, *Y* = 0.35. Pure toluene was added to 13 mL of surfactant solution in 20 mL scintillation vials to attain concentrations of 0–40 mM toluene. The mixtures were agitated overnight. DLS measurements were made after sample filtration (0.2 μm) by (a) a Malvern Instruments (Southborough, MA) Zetasizer Nanosystem SZ or (b) a Brookhaven Instrument (Holtville, NY) system equipped with a 72-channel digital correlator and an argon-ion laser operating at 488 nm.

The distribution of the mean apparent translational diffusion coefficients (*D*_{app}) was determined by fitting the DLS autocorrelation functions using CONTIN and EXSPAM for the Brookhaven instrument. For the Malvern instrument, the autocorrelation functions were fit using “General” and “Multiple Narrow Modes”, both forms of non-negatively constrained least-squares fittings which differ in the parameter used to discriminate signal from noise in the correlogram; “Multiple Narrow Modes”, being an order of magnitude more sensitive to noise, are less reproducible for lower signal to noise ratios. The corresponding apparent hydrodynamic radii were calculated as

$$R_{\text{app}} = \frac{kT}{6\pi\eta D} \quad (1)$$

where *k* is the Boltzmann constant, *T* is the absolute temperature, and *η* is the solvent viscosity in poise. Micelle size is expressed as *d*_{app} = 2*R*_{app}.

Capillary Electrophoresis (CE). Capillary electrophoresis measurements were made on a Beckman P/ACE 2000 Instrument (Fullerton, CA) with UV detection at 254 nm which responded to the chromophores of TX100 and toluene. The 50 μm (i.d.) and

(28) Fillipi, B. R.; Brant, L. W.; Scamehorn, J. F.; Christian, S. D. *J. Colloid Interface Sci.* **1999**, *213* (1), 68–80.

(29) Komesvarakul, N.; Scamehorn, J. F.; Gecol, H. *Sep. Sci. Technol.* **2003**, *38* (11), 2465–2501.

(30) Wang, Y.; Banziger, J.; Dubin, P. L.; Filippelli, G.; Nuraje, N. *Environ. Sci. Technol.* **2001**, *35* (12), 2608–2611.

(31) Stephany, S. M.; Kole, T. M.; Fisch, M. R. *J. Phys. Chem.* **1994**, *98* (43), 11126–8.

(32) Thimons, K. L.; Brazdil, L. C.; Harrison, D.; Fisch, M. R. *J. Phys. Chem. B* **1997**, *101* (51), 11087–11091.

(33) Menge, U.; Lang, P.; Findenegg, G. H. *J. Phys. Chem. B* **1999**, *103* (28), 5768–5774.

(34) Menge, U.; Lang, P.; Findenegg, G. H.; Strunz, P. *J. Phys. Chem. B* **2003**, *107* (6), 1316–1320.

(35) Bettahar, M.; Schafer, G.; Baviere, M. *Environ. Sci. Technol.* **1999**, *33* (8), 1269–1273.

(36) Hill, R. M. In *Mixed Surfactant Systems*; Ogino, K., Abe, M., Eds.; Marcel Dekker: New York, 1993; p 317.

(37) Zhang, B.; Kirton, G. F.; Dubin, P. L. *Langmuir* **2002**, *18* (12), 4605–4609.

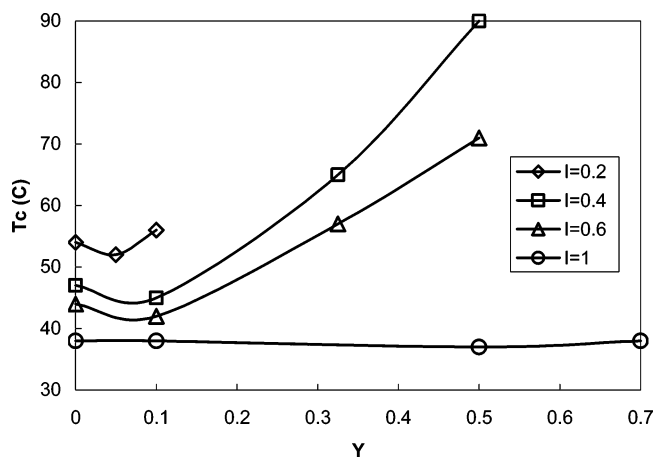


Figure 1. Cloud point temperatures of TX100 as a function of Y (SDS mole fraction) at different ionic strengths.³⁸

20 cm (effective length) capillary was kept at 25 °C. The mobile phase was pH = 9.1, 0.01 M borate buffer combined with 0.49 M NaCl, reaching a total salt concentration of 0.5 M for injection samples in 0.5 M NaCl. For injection samples in 0.1 M NaCl the mobile phase was pH = 9.1, 0.01 M borate buffer combined with 0.09 M NaCl, reaching a total salt concentration of 0.1 M. The voltage was 8 kV for the 0.1 M mobile phases and was reduced to 3 kV for the 0.5 M mobile phase to avoid Joule heating. Mesityl oxide was used as the zero mobility reference material. The total surfactant concentration was 60 mM. The capillary was subjected, between runs, to a 3 min rinse with 0.1 NaOH, water, and buffer.

The electrophoretic mobility was calculated as

$$\mu = \frac{lL}{V} \left(\frac{1}{t_s} - \frac{1}{t_0} \right) \quad (2)$$

where l is the effective length of the capillary, L is the total length of the capillary (cm), V is the applied voltage, and t_0 and t_s are the migration times of the reference marker and the sample, respectively.

Results

Cloud Point. Micelle growth can arise from attractive intermicellar interactions, which for nonionic micelles has been related to cloud point phenomena. Therefore, it was necessary to determine whether the systems studied here were close to the cloud point. Figure 1, from Dubin et al.,³⁸ shows the depression of the TX100 cloud point by ca. 30 °C upon addition of 1 M NaCl. The elevation of the cloud point by addition of SDS is reasonably attributed to intermicellar repulsion, which is effectively screened out in 1 M NaCl, but not at lower ionic strengths; the local minimum at Y (SDS mole fraction) = ca. 0.05 has been discussed.³⁸ At the conditions of the current work, i.e., $Y = 0$ or 0.35, 0.5 M NaCl, and ambient temperature, it is clear that our experiments were carried out at least 20 °C below the cloud point.

Turbidity. Turbidimetric titrations were conducted by addition of pure toluene to TX100 (10, 40, and 60 mM) and to TX100/SDS (15, 30, 60, and 90 mM total surfactant concentration, $Y = 0.35$), in 0.5 M NaCl, with results shown in Figure 2. Since the highest value of the critical micelle concentration (cmc) for all these systems (mixed micelles, 0.5 M NaCl) is less than 0.5 mM,³⁷ we need consider only the micellar state of the surfactant. On the other hand, since the solubility of toluene in water is 5.4 mM, the distribution of toluene between aqueous and micellar phases is not exactly known at low levels of added toluene,

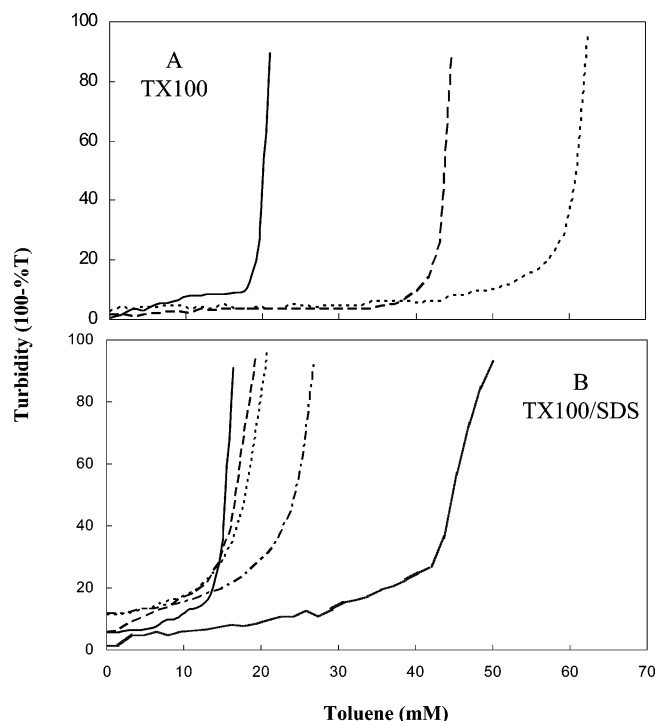


Figure 2. Effect of surfactant concentration on turbidimetric titrations in 0.5 M NaCl with pure toluene: (A) TX100 (10, 40, and 60 mM from left to right); (B) TX100/SDS ($Y = 0.35$, total surfactant 15, 30, 60, and 90 mM, from left to right). Far right: 30 mM TX100/SDS in 0.16 M NaCl.

although DLS results reported below strongly indicate high levels of partitioning into micelles. At high added toluene, its concentration in the nonmicellar aqueous phase may be as large as 5.4 mM. Since this toluene makes no contribution to turbidity, the results of Figure 2 reflect only the solubilized toluene.

Both micellar systems (Figure 2) exhibit a gradual increase in turbidity followed by an abrupt increase, which was observed at higher toluene concentrations for higher surfactant concentrations. The abrupt increase in turbidity appeared at much lower added toluene for the mixed micelle system, with marked sensitivity to ionic strength. Thus, when 30 mM TX100/SDS ($Y = 0.35$) was titrated with toluene, the abrupt enhancement in turbidity which appeared at 45 mM toluene in 0.16 M NaCl diminished to 10–15 mM toluene when the ionic strength increased to 0.5 M NaCl.

When the titration of 10 mM TX100 in 0.5 M NaCl was terminated at the point of the abrupt increase in turbidity (19 mM toluene), the highly turbid solution gradually separated over 3 days into two phases. The upper clear phase (97% of the total volume) consisted of TX100 micelles with a diameter of 24 nm (measured by DLS, see below). The lower turbid phase was rich in TX100 (83% w/w) and toluene droplets were observed upon drying (120 °C). These turbidity results, although intriguing, are difficult to interpret because turbidity depends in a complex matter on the concentration, size, geometry, and polarizability of the scattering particles. For that reason, the system was further characterized by DLS.

Dynamic Light Scattering. Micellar solutions of 60 mM TX100 in 0.5 M NaCl were rapidly mixed with 0–40 mM toluene. After the samples were rocked overnight, the solutions were monophasic. The turbidities of these solutions were measured (Figure 3A), and the average hydrodynamic diameters of the micelles were obtained by two different DLS instruments (with better than 7%

(38) Dubin, P. L.; Principi, J. M.; Smith, B. A.; Fallon, M. A. *J. Colloid Interface Sci.* **1989**, *127* (2), 558–565.

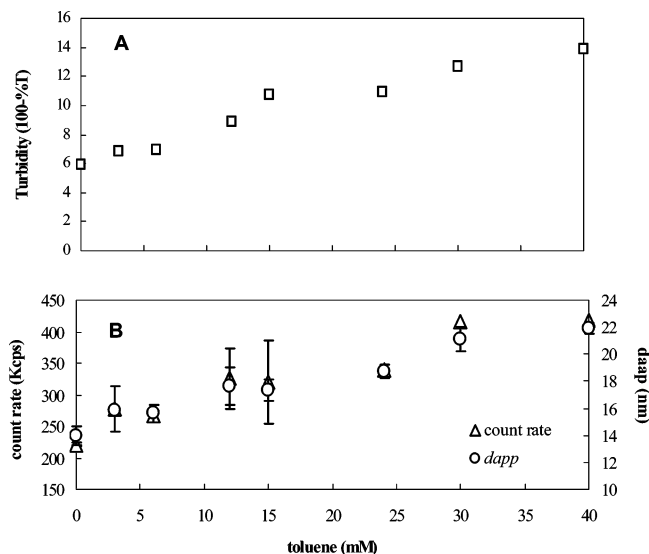


Figure 3. Effect added toluene (0–40 mM) on 60 mM TX100 in 0.5 M NaCl: (A) turbidity (100 – %T); (B) light scattering intensity (count rate), apparent diameter.

Table 1. Effect of Added Toluene (0, 3, and 30 mM) on the Diameters of TX100 Micelles (10, 40, and 60 mM) in 0.5 M NaCl

TX100 (mM)	micelle diameters (nm) measured at indicated toluene concentrations		
	0 mM toluene	3 mM toluene	30 mM toluene
10	11.2 ± 0.1	13.7 ± 0.2	33.0 ± 3.4
40	13.5 ± 0.1	14.4 ± 0.2	33.0 ± 3.8
60	13.9 ± 0.1	14.6 ± 0.2	23.3 ± 1.9

agreement) and the results (Malvern instrument) are shown in Figure 3B. Monomodal distributions were obtained at all toluene concentrations. Micelle diameters correlated well with both count rate and turbidity. The gradual increase in micelle diameter from 14 to 22 nm indicated the swelling of micelles upon toluene addition.

The effect of toluene concentration on micelle size for 10, 40, and 60 mM TX100 in 0.5 M NaCl is shown in Table 1. In the absence of toluene, the effect of surfactant concentration on size was similar to that observed for other nonionic surfactants.³⁹ The apparently anomalous result for 30 mM toluene, for which micelle size decreases at

high TX100 concentrations, will be examined in the discussion section. At all three surfactant concentrations, micelle size was observed to increase with addition of toluene.

The diameters of mixed micelles (total surfactant 60 mM, $Y = 0.35$) in 0.5 M NaCl are shown in Figure 4 as a function of added toluene (0–24 mM). The diameter of toluene-free TX100/SDS (24 nm) is larger than the diameter of TX100 (14 nm) micelles at the same concentration. At high ionic strength, mixed anionic/nonionic surfactants are known to form larger micelles than pure nonionic surfactants.^{12,38} Micelle diameter increased slightly upon the addition of 3 mM toluene, but at higher toluene concentrations (6–24 mM) a dramatic increase in micelle size was observed and size distributions became obviously bimodal. The bimodal distributions were confirmed in several cases by using both instruments (results not shown). The apparent hydrodynamic diameter of both size populations increased with toluene concentration, reaching 140 nm for the large particles.

The large effect of ionic strength for TX100/SDS with toluene (Figure 2B) suggested measurement of micelle diameter in 0.1 M NaCl as a function of toluene, with the results shown in Figure 5.

Capillary Electrophoresis. To clarify the nature of two coexisting species suggested by DLS, electropherograms were obtained as a function of added toluene for TX100/SDS mixed micelles in 0.1 and 0.5 M NaCl, with the results shown in Figure 6. As shown by comparison of systems with and without toluene in Figure 6A, the predominant contributor to the signal is TX100, not toluene. Broad distributions of mobilities were observed in both the presence and absence of toluene, as previously reported for TX100/SDS in the absence of solubilize.³⁷ The breadth of TX100/SDS mobilities decreased with an increase in ionic strength. The decrease in mobility with ionic strength is presumably due to counterion condensation.⁴⁰

The addition of either 3 or 24 mM toluene at 0.5 M NaCl led to the appearance of two mobility ranges: one also present in the toluene-free solution ($0.7-1) \times 10^4 \text{ cm}^2 \text{ V}^{-1} \text{ s}^{-1}$, and an additional low mobility peak ($0.05-0.3) \times 10^{-4} \text{ cm}^2 \text{ V}^{-1} \text{ s}^{-1}$ (Figure 6B). The addition of toluene did not change the electropherograms obtained in low salt, which displayed only peaks attributable to mixed micelles. In all cases, solutions displaying bimodal DLS distributions also yielded two mobility peaks, while a single range of

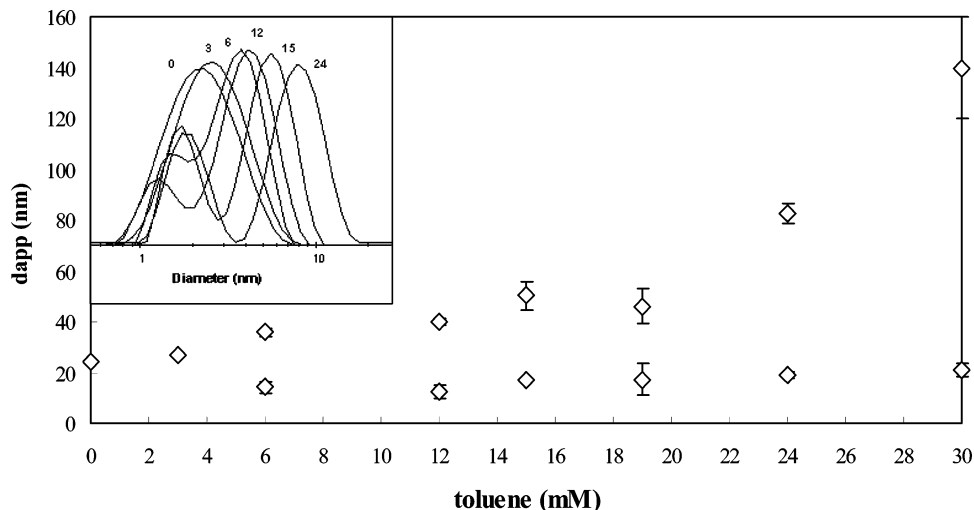


Figure 4. Distributions of d_{app} (Malvern) for TX100/SDS (60 mM total surfactant, $Y = 0.35$, 0.5 M NaCl) for toluene concentrations from 0 to 24 mM (insert); also plotted as mean diameter(s) vs added toluene (double data points correspond to bimodal distributions).

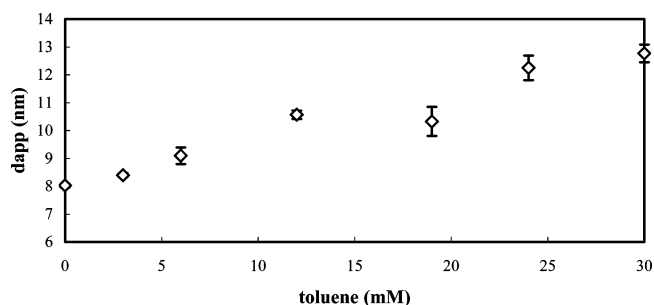


Figure 5. Apparent diameter of TX100/SDS micelles (60 mM, $Y = 0.35$, 0.1 M NaCl) as a function of added toluene (Malvern).

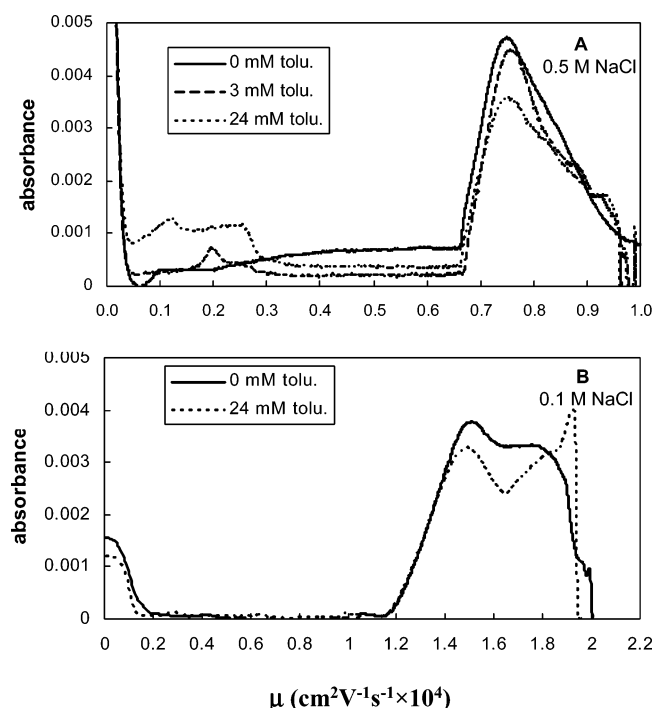


Figure 6. Mobility distribution of TX100/SDS ($Y = 0.35$) micelles with 0, 3, and 24 mM toluene: (A) in 0.5 M NaCl; (B) in 0.1 M NaCl.

mobility was observed for solutions that showed monomodal DLS spectra.

Discussion

The turbidimetric titration curves shown in Figure 2 can be interpreted in terms of solubilization, the initial gradual increase in turbidity corresponding to solubilization-induced micelle swelling. The subsequent abrupt turbidity increase corresponds to phase separation, and its shift to higher toluene concentrations for higher surfactant concentrations suggests that phase separation occurs only after solubilization capacity is exceeded. At fixed total surfactant concentration, both TX100 micelles and mixed micelles at low salt appear to have higher solubilization capacities than mixed micelles at high ionic strength. However, interpretation of turbidity results is limited by their simultaneous dependence on both micelle size and number and also by the nonequilibrium state of the solutions represented by Figure 2. Consequently DLS was used to measure micelle size under equilibrium conditions.

Micelle growth with added toluene is seen most clearly for those systems showing monomodal distributions only, i.e., Figure 3 (TX100 micelles in 0.5 M NaCl) and Figure 5 (mixed micelles in 0.1 M NaCl). Similar micelle growth was reported upon addition of benzene and phenol to anionic and cationic micelles, respectively.^{32,19} The emergence of bimodal distributions as seen in Figure 4 (mixed micelles at 0.5 M NaCl) suggests an unequal distribution of toluene between two micelle populations, which will be further supported by CE results discussed below. In the other cases, we assume an equal distribution of toluene among the micelles. Since the ratio of toluene/surfactant decreases with increased surfactant concentration, the effect of toluene is largest at low surfactant concentration (see Table 1). For example, the addition of 3 mM toluene to 10, 40, and 60 mM TX100 caused d_{app} to increase by 2.5, 0.9, and 0.7 nm (20, 6, and 5%, respectively). The difference in micellar diameter increase among the surfactant solutions was even more pronounced (2-fold) in the presence of 30 mM toluene. However, a plot of micelle size as a function of the toluene/TX100 ratio (not shown) is not linear. Menge et al.³³ also showed that the increase in molar mass of solubilizing micelles does not simply depend on solubilize/surfactant ratio.

Mixed micelle swelling depended not only on toluene and surfactant concentrations but also on ionic strength. For 60 mM total surfactant, addition of 3 mM toluene increased the diameters of the mixed micelles by 0.5 nm in 0.1 M NaCl but, surprisingly, by 2.6 nm in 0.5 M NaCl. This effect can be considered in terms of micelle size and shape.

The mixed micelles at low ionic strength with diameters of 8 nm are evidently spherical and exhibit spherical growth. Since this places an upper limit of about 4 nm for the minor axis of larger micelles, the value of d_{app} 24 nm (i.e., twice the hydrodynamic radius), seen for mixed micelles at high salt indicates a major axis of at least 30 nm (see below and ref 44). These micelles are evidently prolate (i.e., rodlike) and grow by elongation as ellipsoidal micelles do.^{12,41,42} The 6% increase in the spherical micelle size upon addition of 3 mM toluene from 8 to 8.5 nm diameter corresponds to an increase in micelle size due to solubilization $\Delta V_m = 50 \text{ nm}^3$. This can be compared to a calculated $\Delta V_{\text{tol},m} = 1.5 \text{ nm}^3$ obtained from the added toluene volume and the number of micelles in the system estimated from aggregation numbers for spherical micelles.⁴³ The fact that ΔV_m is substantially larger than $\Delta V_{\text{tol},m}$ indicates that the spherical micelle aggregation number increases with toluene solubilization. To obtain ΔV_m for the nonspherical micelles, the measured hydrodynamic diameters were converted to ellipsoidal dimensions using the approach presented in a monograph relating diffusion coefficients and axial dimensions for prolate ellipsoids, based on Perrin's equations, and taking the minor axis to be constant.⁴⁴ ΔV_m in 0.5 M NaCl for mixed micelles and for TX100 micelle due to the addition of 3 mM toluene was 55 and 50 nm^3 , respectively, similar to ΔV_m for spherical micelles. Thus, an increase in the hydrodynamic diameter of only 0.5 nm for spherical micelles corresponds to the same volume change as an increase in hydrodynamic diameter of 2.6 nm for rodlike micelles.

(41) Robson, R. J.; Dennis, E. A. *J. Phys. Chem.* **1977**, *81* (11), 1075–8.

(42) Singh, M.; Ford, C.; Agarwal, V.; Fritz, G.; Bose, A.; John, V.; McPherson, G. *Langmuir*, in press.

(43) Lang, J. *J. Phys. Chem.* **1990**, *94* (9), 3734–9.

(44) Thé, S. Micelle surface potential and light scattering studies of polyion-mixed micelle complexes. Thesis, Purdue University, 1989.

(39) Kato, T.; Kanada, M.-a.; Seimiya, T. *J. Colloid Interface Sci.* **1996**, *181* (1), 149–158.

(40) Treiner, C.; Khodja, A. A.; Fromon, M. *J. Colloid Interface Sci.* **1989**, *128* (2), 416–21.

The difference in shape and consequently in the mode of growth for mixed micelles at low vs high ionic strength may help explain the dramatic increase in micelle size and the unexpected bimodal distribution obtained when toluene is added (6–24 mM) to mixed micelles at high ionic strength. To accommodate high levels of added toluene, rodlike micelles must grow extensively. However, extensive elongation is limited since it is accompanied by a loss of endcaps, regions of high curvature in which the mutually repulsive SDS headgroups are presumably accommodated. Although SDS headgroup repulsion is clearly reduced in 0.5 M NaCl, indirect evidence for the persistence of repulsive forces comes from the increase in cloud point with Y , even in 0.6 M NaCl (Figure 1). We propose that the energetically unfavorable formation of long cylindrical micelle domains rich in SDS is avoided by accommodating excess toluene in microemulsion droplets stabilized mainly by SDS. Migration of SDS from rodlike micelles to microemulsions is supported by mobility measurements reported below. The bimodal distribution therefore may correspond to the coexistence of small mixed micelles and somewhat larger microemulsions stabilized mainly by the high cmc surfactant, SDS. Because TX100 monomers do not require domains of high curvature as much as SDS does, the formation of a microemulsion was not observed with TX100 micelles even at very high toluene concentrations. However, transitions of rodlike micelles in nonmixed systems to microemulsions have been observed and explained by various mechanisms, e.g., for cationic hexadecyltrimethylammonium micelles in the presence of benzene¹⁹ and nonionic C₁₂E₅ in the presence of high decane concentrations.³³

Bimodal distributions in solubilization systems have been reported by Lang⁴³ who measured aggregation numbers of SDS in the presence of 1-pentanol by time-resolved fluorescence, the analysis of which suggested two populations of micelles with different aggregation numbers. Imae et al.⁴⁵ examined hexanol solubilization in cationic/nonionic dodecyldimethylamine oxide micelles and obtained by light scattering the coexistence of 4.4 and 26 nm species which she interpreted as “empty” micelles along with microemulsion droplets of hexanol stabilized by surfactant. In the present case we provide evidence for the coexistence of mixed micelles and microemulsion by CE measurements.

When toluene was added to mixed micelles at high ionic strength a broad peak of low mobilities which was not observed in the toluene-free system appeared in the electropherogram (Figures 6A). This peak at mobilities $(0.05\text{--}0.3) \times 10^{-4} \text{ cm}^2 \text{ V}^{-1} \text{ s}^{-1} \times 10^4$ was attributed to

large and weakly charged (by SDS) microemulsion droplets. The high mobility peaks attributed to the mixed micelles, however, were unchanged upon the addition of toluene (3 and 24 mM). The micelle mobility, to a first approximation, varies as the ratio of charge to friction coefficient and, therefore, varies as the ratio of aggregation number n to radius R_h ; hence, mobility could be insensitive to toluene addition, if both n and R_h increased to the same extent. The ratio of low-mobility to high-mobility peaks increased with toluene concentration, also supporting the identification of the former as microemulsion. Under conditions where DLS monomodal size distributions indicated no microemulsion formation, no low mobilities were observed by CE (Figure 6B). Future studies should focus on separating and characterizing the small “swollen” micelles and larger microemulsion species.

Conclusions

Micelle growth due to toluene solubilization was observed for both nonionic and nonionic/anionic surfactant systems; however, two different modes of growth were observed, depending on the initial size and shape of the micelles. Large rodlike mixed micelles in 0.5 M NaCl grew extensively by elongation to accommodate 3 mM toluene, resulting in a large increase in hydrodynamic diameter; small spherical mixed micelles in 0.1 M NaCl increased by the same volume per micelle while remaining spherical, resulting in a small increase in diameter. At higher toluene concentration, the nonspherical mixed micelles do not exhibit further elongation but split into microemulsions and small swollen micelles. We propose that the limited elongation of nonspherical micelles is due to loss of regions of high curvature in which SDS is presumably accommodated, so that solubilization proceeds by the formation of microemulsion droplets stabilized by SDS.

Understanding solubilization may be complicated by a failure to distinguish between micelle and microemulsion mechanisms. The transition from micelles to microemulsions may be utilized to achieve higher solubilization, but changes in physical properties, such as viscosity and conductivity, must be considered as well. For these reasons the different modes of micelle growth during solubilization need to be taken into account when surfactants are selected for various cosmetic, pharmaceutical, and environmental applications.

Acknowledgment. Support from the Israeli Council for Higher Education, Bekura postdoctoral fellowship, is acknowledged.

(45) Imae, T.; Okamura, H.; Furusaka, M. *J. Colloid Interface Sci.* **1994**, *168* (1), 217–21.